Title

Role Of Infrapatellar Fat Pad Size In Osteoarthritis Progression: Data From The Osteoarthritis Initiative

Authors

Lee, K
Banuls-Mirete, M
Lombardi, AF
et al.

Publication Date

2023-03-01

DOI

10.1016/j.joca.2023.01.296

joint. The subjects were divided into two groups according to 3 mm of MME as a cut-off value with an MME of 3 mm as the cutoff value (nMME: MME<3 mm, pMME: MME ≧ 3 mm). The relationship between the mechanical axis of the lower limb (%MA) and MME was examined using Spearman's rank correlation analysis and simple regression analysis. All analyses were undertaken using the statistical package SPSS version 27.

Results: The severity of radiographic knee OA of the subjects was 16 (1.0%) for K/L 1, 1,025 (86.1%) for K/L 2, 112 (9.4%) for K/L 3, and 38 (3.2%) for K/L 4. The %MA and MME of the subjects were 37.76±13.64 % and 3.90±2.06 mm, respectively. Four hundred sixty one (461) subjects (38.8%) were classified into the nMME group, while the remaining 726 subjects (61.2%) were classified into the pMME group. The age of pMME group (73.36±5.57 years old on average) was significantly higher than that of the nMME group (72.20±5.09 years old on average) (p<0.001). While 201 among 461 subjects (43.6%) were female in the nMME group, 474 among 726 subjects (65.3%) were female in the pMME group. Statistical significance was observed between two group in terms of gender of the subjects (p<0.001). The BMI of the pMME group (23.1±3.04 kg/m^2) was significantly higher in comparison to that of the nMME group (22.4±2.87 kg/m^2) (p<0.001). The severity of radiographic knee OA of the pMME group (66 [9.1%] for K/L 1, 531 [73.1%] for K/L 2, 86 [11.8%] for K/L 3, and 47 [6.5%] for K/L 4) was significantly higher than that of the nMME group (111 [24.1%] for K/L 1, 336 [72.9%] for K/L 2, 13 [2.8%] for K/L 3, and 1 [0.2%] for K/L 4) (p<0.001). The MME of the subjects in the pMME group (5.02±1.85 mm) was significantly greater than that of those in the nMME group (2.12±0.67 mm) (p<0.001). The % MA of the subjects in the pMME group (36.75±14.63 %) was significantly smaller than that of those in the nMME group (39.48±11.68 %) (p<0.001). The correlation coefficient (r) between MME and %MA of the subjects was -0.17 (p<0.001). Although the correlation coefficient (r) between MME and %MA of the subjects in the nMME group was 0.08 (p=0.107), that of those in the pMME group was -0.284 (p<0.001). In a regression analysis, β for the association between MME and %MA was -1.075 (95%CI: -2.11 to -1.39, p<0.001) of the subjects. When the subjects were divided into two groups by the presence of absence of MME, %MA was associated with MME of the subjects in the pMME group (β: -2.765, 95%CI: -3.31 to -2.22, p<0.001), while no association was observed between MME and %MA in the nMME group (β: 1.164, 95%CI: -0.44 to 2.77, p=0.154) in a regression analysis.

Conclusions: The mechanical axis of the lower limb in elderly populations were associated with MME. While when MME was <3 mm, % MA was not associated with MME, %MA was associated with MME when MME was ≧3 mm.

279
IDENTIFICATION OF CD64 AS A MARKER FOR THE DESTRUCTIVE POTENTIAL OF SYNOVITIS IN OSTEOARTHRITIS

I.J. Teunissen van Manen [1], I. Di Ceglie [1], W.F. Theeuwes [1], N.J. van Kooten [1], M.I. Koenders [1], P. Jimenez-Royo [2], P. Laverman [1], P.M. van der Kraan [1], P.L. van Lent [1], A.B. Blom [1], M.H. van den Bosch [1]. [1] *Radboud Inst. for Molecular Life Sci. - Radboudumc, Nijmegen, Netherlands;* [2] *GlaxoSmithKline, Stevenage, United Kingdom*

Purpose: The majority of osteoarthritis (OA) patients present with synovitis, which is associated with increased cartilage degradation. This synovitis is very heterogeneous in terms of extent, cellular composition and the activation state of the cells, which together strongly influences the effects of the inflammation on the surrounding cartilage. Macrophages, especially pro-inflammatory M1-like macrophages, are considered key mediators of joint destruction. Whereas the presence and extent of synovitis can be determined using classical anatomical imaging modalities such as (contrast enhanced) magnetic resonance imaging or ultrasound imaging, this does not provide information about the cellular composition and aggressiveness of the inflammation. Therefore, a molecular marker that characterizes the destructive potential of the synovitis could be a valuable tool to benefit monitoring of disease progression and therapeutic efficacy in OA. CD64 (Fc-gamma receptor I) has previously been highlighted as a marker for activated myeloid cells and is mainly expressed on pro-inflammatory macrophages. Here, we investigated whether CD64 could act as molecular marker to detect the activation state and aggressiveness of the synovitis in OA patients.

Methods: Synovial biopsies were obtained from end-stage OA patients that underwent joint replacement surgery. mRNA expression levels of *FCGR1*, encoding CD64, and OA-related targets was determined using RT-qPCR. CD64 protein expression and localization in the synovial tissue was determined using immunohistochemistry and immunofluorescence and quantified using flow cytometry. Associations between CD64 expression and factors relevant for OA pathology were investigated. Primary OA synovial fibroblasts and articular chondrocytes were incubated with conditioned media produced from synovial biopsies and mRNA expression of proteolytic enzymes was measured with RT-qPCR. Molecular imaging of CD64 was studied using a model for robust synovitis that was established using SCID mice (*CB-17/lcr-Prkdcscid/Rj*) that were subcutaneously xenografted with inflamed synovial tissue from end-stage RA patients, followed by intravenous injections with dually labelled [^{111}In]In-DTPA-IRDye 800CW anti-CD64 antibody or isotype control antibodies. Targeting was evaluated by biodistribution assessment, μSPECT/CT and IVIS imaging analysis.

Results: Immunohistochemical and immunofluorescence staining confirmed the presence of CD64 in human OA synovium and showed a wide range in CD64 expression levels and localization among the different patients. In some patients the CD64 positive cells were predominantly present in the lining layer, whereas others showed a more diffuse staining. Interestingly, *FCGR1* gene expression positively and significantly correlated with the expression of the pro-inflammatory factors *S100A9*, *IL1B* and *IL6*. Moreover, significant positive associations were measured between *FCGR1* and the expression of the catabolic factors *MMP1*, *MMP3*, *MMP9* and *MMP13*. On protein level, CD64 expression was mainly present on CD45+ leukocytes and correlated with expression of *MMP1*, *MMP3* and *MMP13*, but not with pro-inflammatory cytokines. Finally, we observed that synovial CD64 protein levels in tissue from which conditioned media were made, significantly associated with the induction of *MMP1*, *MMP3* and especially *ADAMTS4* expression in primary OA synovial fibroblasts, but not primary OA articular chondrocytes. In another research line, we established a molecular imaging modality for CD64 using the synovium-SCID xenograft model, which was intravenously injected with dually labelled [^{111}In]In-DTPA-IRDye 800CW anti-CD64 antibody and isotype control. This showed a significantly higher uptake ratio of the anti-CD64 antibody in the synovial explants over blood when compared to the isotype. Moreover, injecting an excess of unlabeled antibody reduced the antibody-binding associated signal, which indicated specific receptor binding.

Conclusions: Our results indicate that synovial CD64 expression is associated with the production of proteolytic enzymes and inflammatory markers related to structural damage in OA. CD64 therefore holds promise to be used as marker to characterize the activation state and damaging potential of synovitis and as such might be used as a tool to monitor disease progression and test the effects of novel therapeutic agents in OA using the synovium-SCID xenograft model we set up.

280
ROLE OF INFRAPATELLAR FAT PAD SIZE IN OSTEOARTHRITIS PROGRESSION: DATA FROM THE OSTEOARTHRITIS INITIATIVE

K. Lee [1], M. Banuls-Mirete [1], A.F. Lombardi [1], A.I. Posis [1], E.Y. Chang [1], N.E. Lane [2], **M. Guma** [1]. [1] *Univ. of California San Diego, La Jolla, CA;* [2] *Univ. of California Davis, Sacramento, CA*

Purpose: Prior studies have reported contradictory results on the role of fat pads in osteoarthritis progression. This study aimed to determine the predictive value of infrapatellar fat pad (IPFP) size and its association with obesity in osteoarthritis (OA) progression.

Methods: A case-control study was performed using osteoarthritis initiative (OAI) dataset. 315 cases were right knees with an increase of ≥1 Kellgren-Lawrence score (KL) from baseline to 48 months with 315 controls being those with no KL change were compared. Cases and controls were matched by age, sex, race, and baseline KL. MRI Osteoarthritis Knee Score (MOAKS) was used to score synovitis of IPFP at baseline and 24 months. Cross sectional area (CSA) of IPFP at baseline and 24 months was calculated in the mid-slice of sagittal plane. Subcutaneous fat around the distal thigh (SC fat) was measured by taking the sum of the thickest portion of each of the four quadrants. Adjusted conditional logistic regression was used to determine the odds ratios (ORs) of these imaging markers for radiographic OA progression.

Results: The mean age was 61 years, 70.8% were women, and 87% were White. At baseline, BMI and synovitis scores were significantly higher in cases, while IPFP CSA and SC fat were not. At 24 months, all these 4 imaging markers showed significant increases in cases compared to controls with changes over 24 months also being significantly higher in

Table 1. Baseline values of imaging markers and their changes over time

Baseline values	Case (n=315, mean ± SD)	Control (n=315, mean ± SD)	*P*
BMI (kg/m^2)	29.09±4.69	28.1±4.83	0.014
IPFP CSA (cm^2)	6.51±1.17	6.54±1.17	0.787
SC fat	5.68±2.09	5.50±1.86	0.251
Abdominal circumference (cm)	103.90±12.82	100.95±12.62	0.004
*Hoffa synovitis	0.78±0.72	0.44±0.54	<0.001
*Effusion synovitis	0.71±0.67	0.41±0.51	<0.001
Values at 24 months	**Case (n=284, mean ± SD)**	**Control (n=284, mean ± SD)**	***P***
BMI (kg/m^2)	29.33±5.07	28.20±4.90	0.006
IPFP CSA (cm^2)	6.96±1.20	6.23±1.11	<0.001
SC fat	6.54±2.05	5.87±1.88	<0.001
Abdominal circumference (cm)	105.16±13.43	102.11±12.26	0.004
*Hoffa synovitis	1.25±0.71	0.32±0.47	<0.001
*Effusion synovitis	1.39±0.74	0.37±0.49	<0.001
Change over 24 months	**Case (n=284, mean ± SD)**	**Control (n=284, mean ± SD)**	***P***
Δ BMI (kg/m^2)	0.22±1.76	0.14±1.95	0.633
Δ IPFP CSA (cm^2)	0.47±0.54	-0.27±0.43	<0.001
Δ SC fat	0.84±1.36	0.38±1.19	<0.001
Δ Abdominal circumference (cm)	1.40±9.32	1.33±9.67	0.934
Δ *Hoffa synovitis	0.45±0.84	-0.13±0.5	<0.001
Δ *Effusion synovitis	0.67±0.77	-0.06±0.52	<0.001

BMI: body mass index, IPFP CSA: cross sectional area of infrapatellar fat pad, SC fat: subcutaneous fat assessment around distal thigh, *: Hoffa synovitis and effusion synovitis were scored based on MOAKS

Table 2. Correlations between changes of imaging marker over 24 months

Variable	Variable	Pearson Coefficient	P
Δ BMI	Δ IPFP CSA	0.067	0.111
Δ BMI	Δ SC fat	0.287	<0.001
Δ BMI	Δ Hoffa's synovitis	-0.059	0.159
Δ BMI	Δ Effusion synovitis	0.06	0.153
Δ BMI	Δ Abdominal circumference	0.373	<0.001
Δ IPFP CSA	Δ SC fat	0.103	0.014
Δ IPFP CSA	Δ Hoffa synovitis	0.286	<0.001
Δ IPFP CSA	Δ Effusion synovitis	0.367	<0.001
Δ IPFP CSA	Δ Abdominal circumference	0.051	0.225
Δ SC fat	Δ Hoffa synovitis	0.003	0.948
Δ SC fat	Δ Effusion synovitis	0.153	<0.001
Δ SC fat	Δ Abdominal circumference	0.127	0.003
Δ Abdominal circumference	Δ Hoffa synovitis	-0.084	0.046
Δ Abdominal circumference	Δ Effusion synovitis	0.072	0.087
Δ Hoffa synovitis	Δ Effusion synovitis	0.383	<0.001

BMI: body mass index, IPFP CSA: cross sectional area of infrapatellar fat pad, SC fat: subcutaneous fat assessment around distal thigh

cases (Table 1). Changes over 24 months from baseline for IPFP CSA, SC fat, abdominal circumference, and synovitis scores were significantly correlated (Table 2). Overall, there were no significant sex differences in outcomes except that women had significant differences in BMI and abdominal circumference between cases and controls while men did not. Adjusted ORs (95% CI) for radiographic OA progression controlling for age, sex, baseline BMI, and synovitis scores were 48.71 (16.50-143.75) for IPFP CSA change over 24 months, 28.19 (11.35-69.97) for Hoffa synovitis change over 24 months, 23.86 (9.77-58.24) for effusion synovitis score change over 24 months, 1.33 (1.10-1.61) for SC fat change over 24 months, and 1.06 (1.01-1.09) for baseline BMI.

Conclusions: Radiographic OA progression was associated with 24-month changes of IPFP size and SC fat, and worsening synovitis. The increase in IPFP size over 24 months, but not baseline the value, may be a strong indicator of subsequent radiographic OA progression and is correlated with indicators of obesity, especially with SC fat.

281
CARTILAGE DISPLACEMENT AND STRAIN MAPPING VIA MRI IN AN INITIAL ACL-RECONSTRUCTED PATIENT COHORT

E.Y. Miller, H. Zhu, W. Lee, C.P. Neu. *Univ. of Colorado at Boulder, Boulder, CO*

Purpose: Osteoarthritis (OA) is a degenerative joint disease that is a leading cause of joint pain, disability, and health care costs worldwide. However, diagnosing early-stage OA can be difficult due to a lack of validated outcome measures for individuals with early knee OA. As post-traumatic OA may progress from an initial injury in the superficial zone of cartilage, often due to ligament damage, to more widespread biochemical and mechanical changes throughout the zonal tissue cartilage, quantifying cartilage mechanical properties non-invasively *in vivo* is of substantial interest.

MRI is unique among imaging tools as it can characterize tissues with high spatial resolution, has a deep penetration depth, and can assess tissues non-invasively. Recently, spiral displacement encoding with stimulated echoes (spiral DENSE) MRI has been used to calculate pixel-level full-field displacement maps of soft tissues under repetitive motion. In this work, we coupled spiral DENSE MRI to displacement under applied loading MRI (dualMRI) to capture *in vivo* displacement and mechanical strain maps of the human knee during varus loading in a young and healthy cohort. We then applied this technique to a small cohort of patients who recently experienced an ACL reconstructive surgery, our first application of this technique in a clinical population.

Methods: *Subjects:* Patients who had received an ACL reconstructive surgery (ACLR) between 4 and 7 months prior to the scan date were recruited under IRB-approved protocols (n = 7, 5 females and 2 males). Average subject age was 27.4±3.9 and subjects had a mean BMI of 24.5±3.0. An age, sex, and BMI-matched group of healthy subjects with no history of knee pain or surgery were also recruited (n = 7, 5 females and 2 males). Average subject age in the healthy cohort was 26.1±2.8 years old and subjects had a mean BMI of 23.6±2.7. As BMI and age were slightly lower in the control group, a paired t-test was performed to determine that there were no significant differences in age or BMI between both groups.

Loading Protocol of Human Knee: An MRI-compatible loading apparatus that provides a varus load to the tibiofemoral cartilage of the knee was manufactured and validated, leading to compression of the medial femoral condyle. Moment conservation was used to calculate the load applied on the foot to be equivalent to one-half body weight of load applied at the medial condyle. Subjects were imaged in a clinical MRI system (3T; Siemens Prisma^{fit}) using a cyclic loading regime (pneumatic, 1s load,1s unload) to mimic a walking cadence.

Spiral DENSE MRI Scanning Protocol: Spiral DENSE MRI was collected following preconditioning to a quasi-steady-state load-displacement response. A steady-state response was achieved by applying 8 minutes of cyclic loading to minimize the viscoelastic response of articular cartilage. 27 time-sequenced coronal plane DENSE MR images were collected using 8 averages, 10 spiral interleaves, at a temporal resolution of 40ms. Echo time (TE) was 2.5ms and relaxation time was 20ms. Field of view, slice thickness, and displacement encoding gradient were 160×160mm^2, 1.7mm and 0.64cycles/mm, respectively. Total imaging time was 13.6 minutes.

Data Analysis: The medial cartilage region of interests (ROI) was manually segmented. MRI phase data was unwrapped using a custom Goldstein branch-cut phase unwrapping algorithm. Displacements for each pixel within the cartilage ROIs were determined from unwrapped phase data and smoothed using LOWESS in Matlab. In-plane Green-Lagrange strains were calculated from the smoothed displacements. Paired t-tests were used to determine the significance between control and ACLR groups for all displacements and strains.

Results: The knee joint translated in both *x* and *y* due to varus loading applied at the foot. Average *x* displacements in the medial cartilage

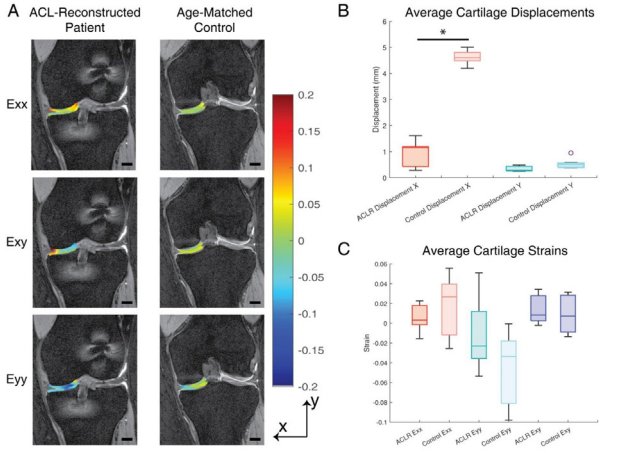

Figure 1. Comparison of DENSE strains and displacements between healthy cohort and patients with prior ACL reconstruction. Representative strain maps for an age-matched ACL-reconstructed patient (ACLR) and control patient are shown in (A). A more disorganized strain pattern with non-zero strains is seen in the ACL-injured patient, while the uninjured patient displays more uniform strain. Average *x* displacements in the medial chondyle were significantly different (p<0.001, paired t-test) between the ACLR and control groups (B). No significant differences were found in average strain values, although more disorganized strain patterns were seen in the ACLR cohort (C). N = 7 (5 female and 2 male) for each cohort. Scale bars indicate 10 mm.